The diagnostic capability of iron lines

Teresa Giannini[a], Brunella Nisini[a], Simone Antoniucci[a], Juan Alcalà[b], Francesca Bacciotti[c], Rosaria Bonito[d,e], Linda Podio[f], Beate Stelzer[d], Emma Whelan[g]

a) - INAF - Osservatorio Astronomico di Roma, Monte Porzio Catone, Italy; b) INAF -- Osservatorio Astronomico di Capodimonte, Napoli, Italy; c) INAF -- Osservatorio Astrofisico di Arcetri, Firenze, Italy d) INAF -- Osservatorio Astronomico di Palermo, Palermo, Italy; e) Università di Palermo, Palermo, Italy; f) Institut de Planetologie et d' Astrophysique de Grenoble, Grenoble, France; g) Institut für Astronomie and Astrophysik, Tübingen, Germany

1. Context

We present the **VLT/X-Shooter spectrum of two jets** from pre-main sequence stars of different luminosity and mass, **ESO-Hα 574 and Par-Lup 3-4.** In the covered spectral range (350-2500 nm) we **detected more than 70 [FeII] and [FeIII] lines.**

The diagnostic capability of iron represents a unique tool to precisely probe the key physical parameters of the gas (electron density and temperature, ionization degree, visual extinction), because:

- The **large number of lines in the ultraviolet-infrared** range makes it possible to trace the physical conditions in a **large range of the parameter space;**
- At variance with the diagnostics commonly performed with other species, such as oxygen, nitrogen, and sulphur, **no assumption on the relative abundance is needed**, since all the parameters are derived from line ratios of the same species;
- In the unperturbed ISM, iron is locked on the grain surfaces, while it is released in gas-phase if gas-grain or grain-grain collisions occur within a shock. Therefore the **iron abundance** (derivable from ratios of iron lines with those of other volatile species) **is a direct probe of the presence of dust** in the jet beam, an information crucial to understand whether jets originate close to the star or in the the dusty regions of circumstellar disks.

2. Spectra and Grotrian diagrams

SPECTRA: UVB (left) and VIS/NIR spectra (right) of ESO-Hα 574 (black) and Par-Lup 3-4 (red) where iron lines are detected. Green, blue, magenta labels indicate [FeII], [FeIII] and blended lines, respectively. For clarity, the spectrum of Par-Lup 3-4 was augmented by a factor of 5.
GROTRIAN DIAGRAMS of Fe^+ (upper panel) and Fe^{++} (lower panel). Blue : ultraviolet lines; green : optical lines, red: near-infrared lines.

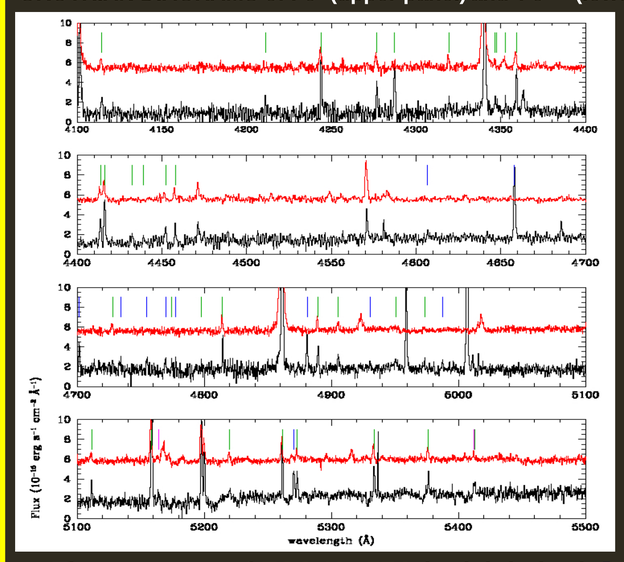

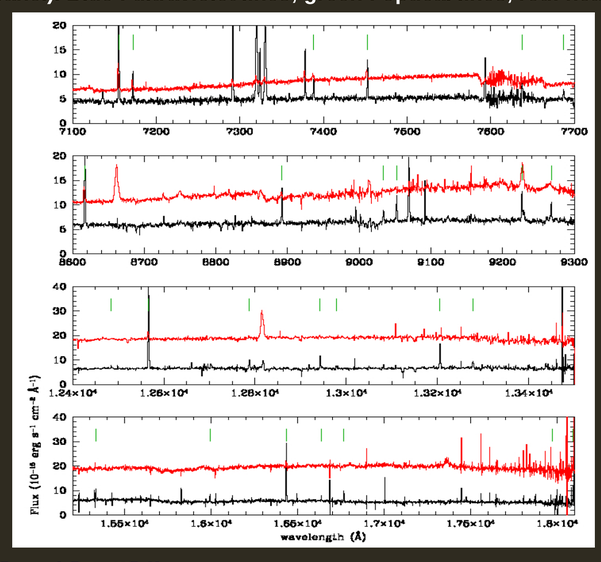

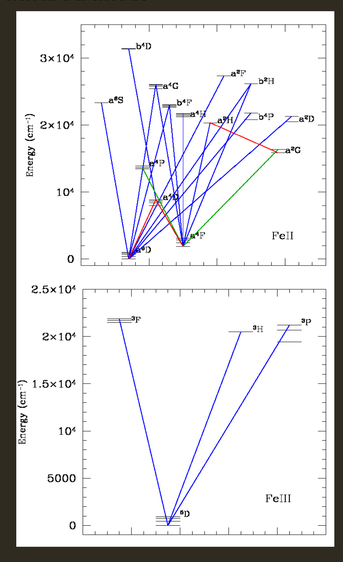

- The spectrum of **ESO-Hα 574** is rich in both **[FeII] and [FeIII] lines**
- The spectrum of **Par-Lup presents only [FeII] lines**
- **In Par-Lup the most excited lines are brighter than in ESO-Hα 574, thus reflecting a higher gas temperature.**

3a. The excitation model : [FeII] lines

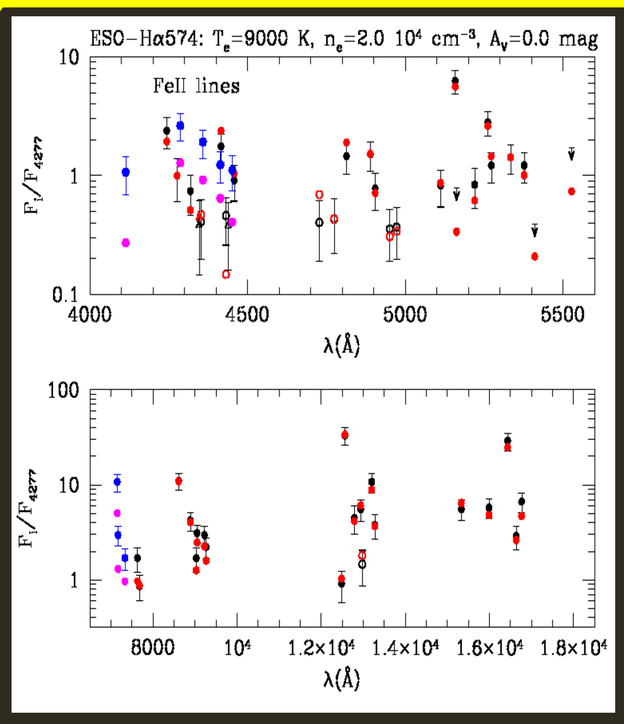

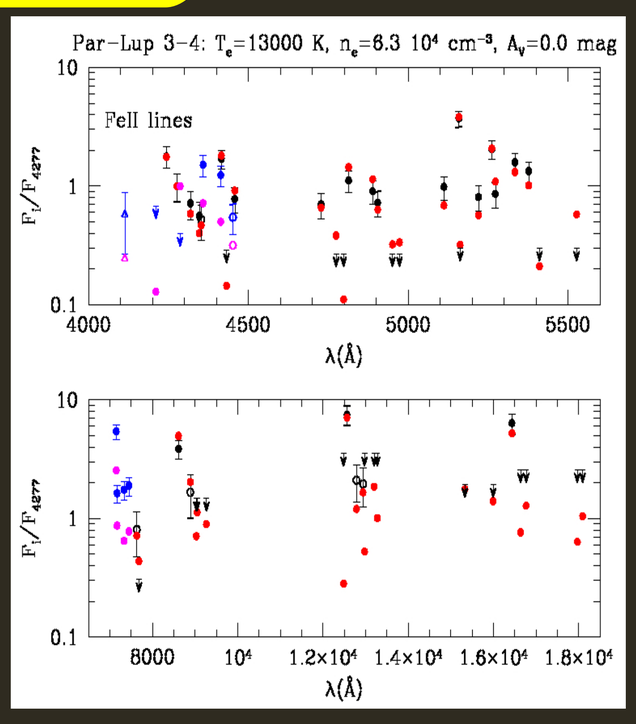

Non Local Thermal Equilibrium (NLTE) best fit model of [FeII] lines detected in ESO-Hα 574 (left) and Par-Lup 3-4 (right). Lines with snr ≥ 5 (filled circles , black: data, red: model) are included the in the fitting procedure. Lines with 3≤ snr ≤ 5 and 2≤ snr ≤ 3 are indicated as open circles and open triangles, respectively. Down arrows are 1-σ upper limits or blended lines. Blue and magenta filled circles refer to lines coming from levels for which the atomic data are poorly known (and therefore not well fitted, Bautista et al. 2013, ApJ, 770, 15).

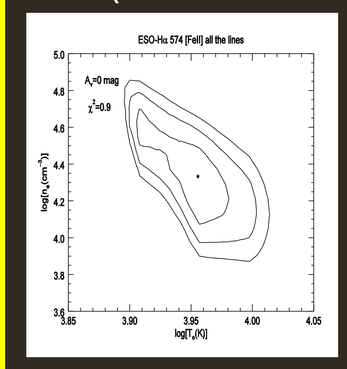

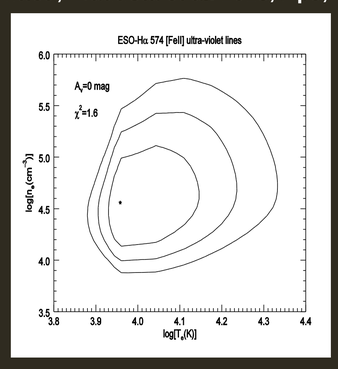

X^2 contours of the fit through the [FeII] lines detected in ESO-Hα 574 (left: all lines, right: ultra-violet lines). The curves refer to increasing X^2 of 30%, 60%, 90%.

- The observed line ratios have been interpreted by means of a NLTE model (159 levels, data taken from the XSTAR database, Bautista & Kallman 2001, ApJS, 134, 139).
- **The ESO-Hα 574 jet is, on average, colder (T_e ~ 9000 K) and less dense (n_e ~ 2 10^4 cm^{-3} than the Par-Lup 3-4 jet (T_e ~ 13000 K, n_e ~ 6 10^4 cm^{-3}).**
- As shown in the contour plot, **a more compact component (n_e up to $10^{5.8}$ cm^{-3}) inside the jet beam is revealed in ESO-Hα 574** jet if the ultra-violet lines are fitted separately. This component is likely the same responsible for the [FeIII] emission (see Sect. 3b).

3b. The excitation model : [FeIII] lines

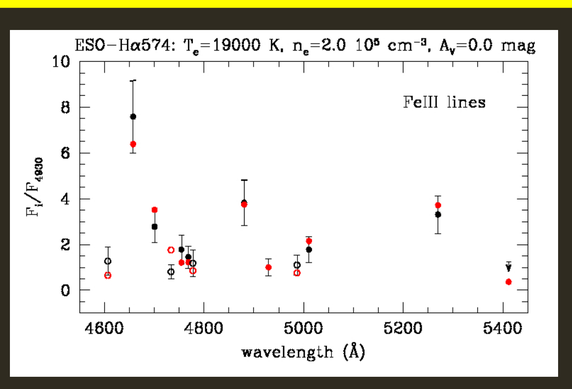

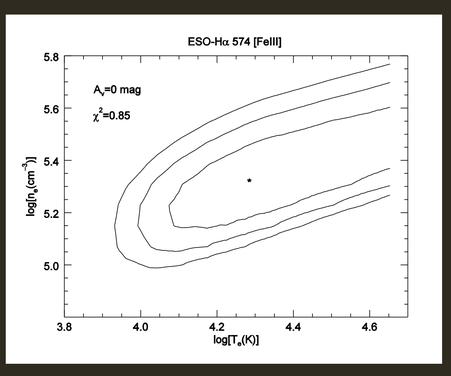

- The observed line ratios have been interpreted by means of a NLTE model (34 levels, data taken from the XSTAR database)
- The best fit model gives T_e ~ 19000 K and n_e ~ 2 10^5 cm^{-3} . **Therefore a density gradient does exist inside the jet beam with the [Fe III] and the [FeII] ultra-violet lines tracing the denser gas component.**

4. The ionization model

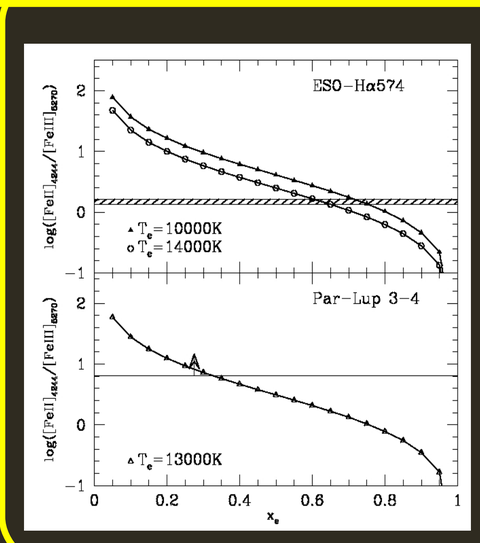

- To consistently interpret the [FeII] and [FeIII] emission and to derive the fractional abundance Fe^+ / Fe^{++} we applied a **ionization equilibrium code for the 4 ionization stages of iron**
- Processes considered : direct ionization, radiative and dielectronic recombination, direct and inverse charge-exchange.
- The fractional ionization $x_e = n_e/n_H$ is derived from severall UV [FeII]/[FeIII] line ratios
- **For ESO-Hα 574 we get 0.65 ≤ x_e ≤ 0.75, while for Par-Lup 3-4 we estimate x_e ≤ 0.25.**

5a. Comparison with shock models

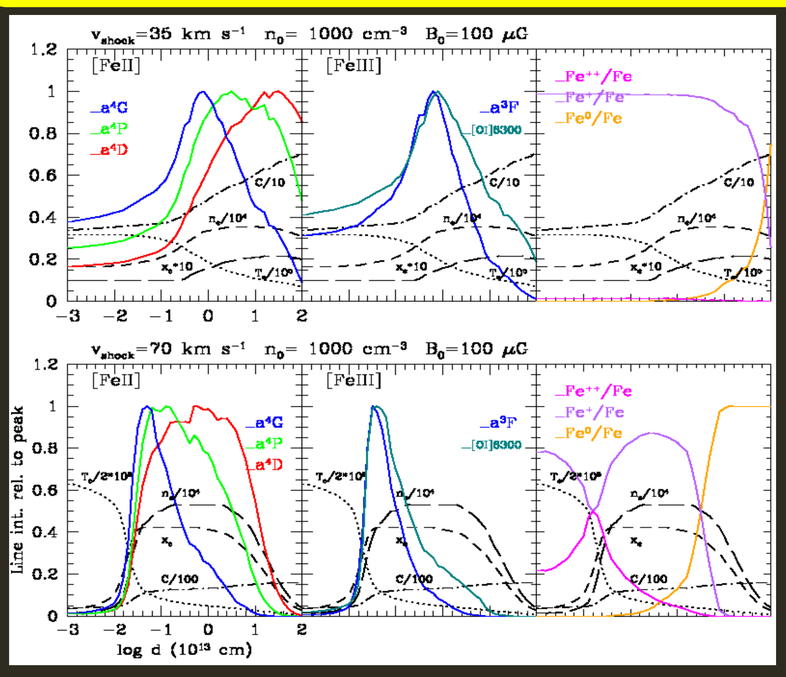

[FeII] and [FeIII] post-shock line intensities (blue: UVB, green: VIS, red: NIR) relative to peak values vs. distance from the shock front (adapted from Hartigan et al. 1994, ApJ, 436, 125). Two shock models (35 km s^{-1} and 70 km s^{-1}) are shown. The right panels give the fraction of Fe^0, Fe^+ and Fe^{++} along the shock profile.

- The physical parameters derived in ESO-Hα 574 and in Par-Lup 3-4 have been compared with the predictions of shock models.
- **Lines at decreasing wavelengths trace progressively higher temperatures.**
- **Increasing shock velocities correspond to decreasing averaged post-shock temperatures and to increasing ionization fractions. This points towards a higher shock velocity in ESO-Hα 574 than in Par-Lup 3-4.**
- The [FeII] ultra-violet and [FeIII] lines trace the portion of the post-shock region close to the shock front, where the density is higher.
- The above scenario is consistent with the detection of [FeIII] lines in ESO-Hα 574 only and with the lack of any line of neutral iron.

5b. Gas-phase abundance

- The gas-phase iron abundance δ(Fe) was derived from the ratios of [FeII] ultra-violet lines with the [OI] 6300 Å. For solar Fe and O abundances, we get **δ(Fe) =0.55 and δ(Fe) =0.25 for ESO-Hα 574 and Par-Lup 3-4 , respectively.**

6. Comparison with diagnostics of other atoms

Ratio	ESO-Hα 574	Par-Lup 3-4
	T (K)	T(K)
[OI]6300/5577	10 000	9 000
[NII]6585/5754	20 000	>17 000
[SII]6716/4068	12 000	>20 000
	n(cm^{-3})	n(cm^{-3})
[OII]3732/7322	2 10^5	8 10^5
[NI]5200/10400	1 10^3	>10^4
[SII]6716/6731	5 10^3	>10^4

The gas diagnostic derived from iron lines has compared with that obtained from other bright lines of oxygen, nitrogen and sulphur.

The main limitation of the diagnostics derived from these lines is their different sensitivity to the variations of the physical parameters (due to their specific excitation energy and critical density).

- The rich iron spectrum from UV to NIR is conversely well suited to obtain a more complete view of the post-shock cooling region.

7. Conclusions

- This work demonstrates that a multiline Fe analysis can be effectively used to probe the excitation conditions of jet beams without any assumption on ionic abundances.
- The **main limitation on the diagnostics resides in the large uncertainties of the atomic data**, which, however, can be overcame through a statistical approach involving many lines
- **A wide spectral coverage, as that of X-Shooter, is mandatory** to get a complete and comprehensive diagnostics.